AD-A073 952 RCA LABS PRINCETON N J F/G 20/12
NEAR AND FAR-FIELD ANALYTICAL APPROXIMATIONS FOR THE FUNDAMENTA--ETC(U)
1978 D BOTEZ DAAG29-77-C-0021
UNCLASSIFIED ARO-14755.5-EL NL

1 OF 1
AD A073952

END
DATE FILMED
10-79
DDC

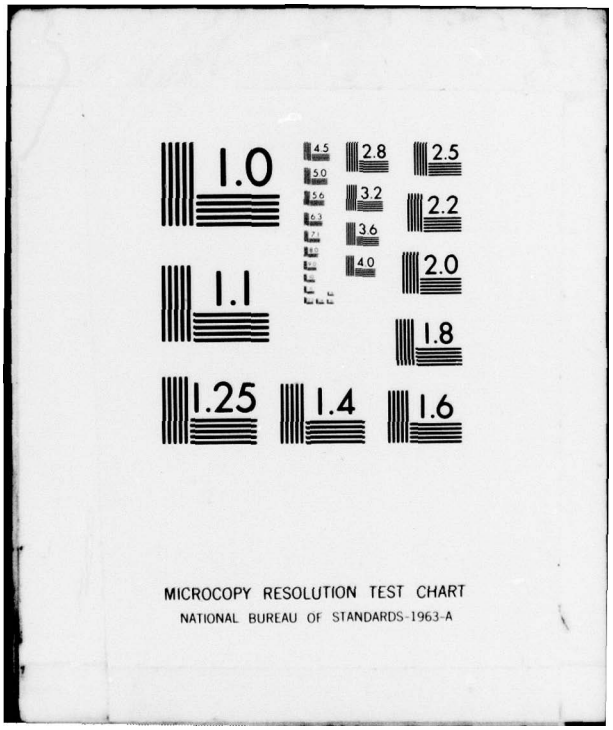
1.0
1.1
1.25
1.4
1.6
1.8
2.0
2.2
2.5
2.8
3.2
3.6
4.0
4.5
5.0
5.6
6.3
MICROCOPY RESOLUTION TEST CHART
NATIONAL BUREAU OF STANDARDS-1963-A

Near and Far-Field Analytical Approximations for the Fundamental Mode in Symmetric Waveguide DH Lasers*

(10) Dan Botez

RCA Laboratories, Princeton, N.J. 08540

Abstract—Analytical approximations of near- and far-field parameters characterizing the TE_0 mode propagation in symmetric double-heterojunction waveguides are described. By using trigonometric function approximations, the mode phase shift at the dielectric interface is estimated within a few percent over the whole range of D (normalized waveguide thickness) variation; as a result, approximations within 1% are obtained for: the field intensity in the waveguide, the effective waveguide thickness, and the effective waveguide index. Field intensity maxima and effective thickness minima are found to occur for $D \cong 1.74$. The physical significance of the approximated parameters to device behavior is discussed. Simple approximation formulae for the radiation confinement factor, Γ_0, of the TE_0 mode (symmetric and asymmetric guide) and TM_0 mode (symmetric guide) are also given. Gaussian approximations are used for estimating near- and far-field intensity profiles over intermediate D ranges ($1.8 < D < 6$ and $1.5 < D < 6$, respectively) and for $\Delta n/n \leq 10\%$. The laser beamwidth in the transverse direction, $\theta_\perp$, is obtained with 4% maximum error by using a Gaussian approximation for $1.5 < D < 5$, and a corrected asymptotic formula for $0 < D < 1.5$. An accurate analytic approximation is also obtained for the laser transverse far-field pattern in the non-Gaussian region $0 < D < 1.5$, $\theta_\perp < 40°$.

1. Introduction

Semiconductor lasers of the double-heterojunction (DH) type have been extensively analyzed[1–3] due both to scientific interest as well as to their utility in a wide range of applications. A DH laser is usually represented as a three-layer slab dielectric waveguide (see Fig. 1) composed of an

* This research was sponsored in part by the U.S. Army Research Office, Durham, N.C., and in part by RCA Laboratories, Princeton, N.J.

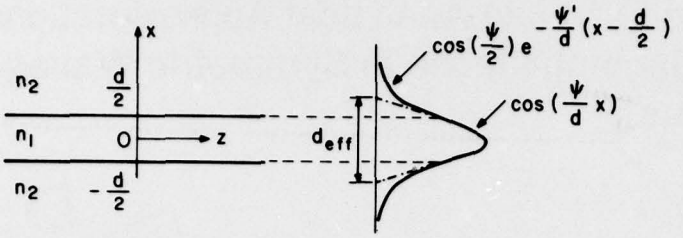

Fig. 1—Schematic representation of the fundamental transverse mode in symmetric double-heterojunction waveguides. The refractive indices of the active layer and cladding layers are n_1 and n_2, respectively, with $n_1 > n_2$. The effective guide thickness $d_{eff} = d(1 + 2/\psi')$.

active layer of refractive index n_1 and thickness d, sandwiched between passive cladding layers of refractive indices n_2 and n_3, respectively, which are less than n_1 (at the lasing wavelength). For symmetric structures (i.e., $n_2 = n_3$), the waveguide has zero cut-off thickness for the fundamental transverse mode.[4,5] In practice, the active layer thickness d is chosen such that only the fundamental mode lases.[1,2] Also the lasing mode is found in most instances to be TE polarized. Thus the symmetric DH operating in the fundamental TE_0 mode is currently the most widely used laser structure for optical communications via fibers. For this reason we chose to restrict most of our analysis to the TE_0 mode. We have reported previously[6] on beamwidth approximations for these structures. In this paper we present a complete description of the fundamental TE_0 mode (near-fields and far-fields) with the help of accurate analytical approximations. The approximations are based both on mathematical properties of certain functions as well as on physical trends in the mode behavior.

The analytical approximations that are employed, while covering wide ranges of parameter variation, have different forms over different intervals rather than a single form resulting from an asymptote combination.[7–9] For this reason we shall refer to our approximation formulae as analytical approximations over intervals (the number of intervals for a given function does not exceed two). Similar approximation methods have been used previously for Fermi energy calculations.[10]

The first part of the paper is concerned with the mode characterization in the near-field. By using approximations for the mode phase shift at the dielectric interface, ψ, various parameters directly dependent on ψ can be accurately determined (e.g., the effective waveguide index). A Gaussian approximation is obtained for near-field distributions over the range $1.8 < D < 6$ ($D \equiv (2\pi/\lambda)d\sqrt{n_1^2 - n_2^2}$ is the normalized guide thickness[4]). In the second part, a Gaussian approximation is used for describing fields in the far-field over the range $1.5 < D < 6$. The Gaussian

approximation for this interval, as well as an asymptotic approximation for the range $0 < D < 1.5$, allows a very precise (within 4%) computation of the beam angular spread in the plane perpendicular to the junction, $\theta_\perp$ (fwhp). Relatively simple expressions for the far-field intensity patterns are also presented.

2. Mode Propagation in the Waveguide

The propagation of the TE_0 mode in the symmetric waveguide of Fig. 1 is characterized by the following variation of the electric field:[4]

$$E_y(x,z) = E_0\{\cos(qx)\}e^{-j\beta z} \quad \text{for } |x| < d/2$$

$$E_y(x,z) = E_0\{\cos(qd/2)\exp[-p(|x| - d/2)]\}e^{-j\beta z} \quad \text{for } |x| > d/2. \quad [1]$$

Here q and p are "transverse propagation constants" in the active layer and cladding layer, respectively, β is the propagation constant along the z direction, and E_0 is the amplitude of the $E_y(x,z)$ field component. The field time dependence is omitted. After applying the proper boundary conditions one obtains the mode equation,[5]

$$\psi \tan\left(\frac{\psi}{2}\right) = \psi', \quad [2a]$$

where $\psi = qd$ and $\psi' = pd$; ψ and ψ' are related by the condition

$$\psi^2 + \psi'^2 = \left(\frac{2\pi d}{\lambda}\right)^2 (n_1^2 - n_2^2) = D^2, \quad [2b]$$

where D is the normalized waveguide thickness.[4] For the fundamental mode, the quantity ψ is identical to the phase shift suffered by the guided wave at the dielectric interface upon total internal reflection.[11] For this reason we shall refer to ψ as phase shift at dielectric interface. Eqs. [2a] and [2b] reduce to

$$\frac{\psi}{\cos\left(\frac{\psi}{2}\right)} = D. \quad [2c]$$

All the information on a given structure is obtained in D, and thus Eq. [2c] unequivocally determines the phase factor ψ characteristic of the TE_0 mode propagation in the structure. In Fig. 1 we also show the electric field variation with x: the electric field follows a $\cos[(\psi/d)x]$ dependence in the active layer, and an exponential $\exp[-(\psi'/d)(|x| - d/2)]$ dependence in the cladding. The electric field amplitude E_0 is obtained by normalizing the fields to unity:

$$\int_{-\infty}^{\infty} E_y(x,z)E_y^*(x,z)dx = 1. \quad [3a]$$

The result is

$$E_0 = \frac{1}{\sqrt{d(0.5 + 1/\psi')}} = \frac{1}{\sqrt{0.5d + 1/p}} = \sqrt{\frac{2}{d_{eff}}} \qquad [3b]$$

where d_{eff}, the effective guide width, is the sum of d and the penetration depths ($1/p$ for each cladding layer), as shown in Fig. 1. The electric field variation, as shown in Fig. 1, is an exact description of the mode in the guide. Strictly speaking, it is not identical to the laser near-field distribution, due to incident power coupling to unguided radiation modes at the laser facet.[12,13] However, this difference has been shown to be negligible in semiconductor lasers,[12,13] and thus we shall consider the field description given by Eqs. [1] as applying to the near-field distribution as well.

Another useful parameter in describing the dielectric waveguide is the effective waveguide index N.[11,14]

$$N = \frac{\beta}{k_0} = \frac{\beta}{\left(\frac{2\pi}{\lambda}\right)} = \sqrt{n_2^2 + \left(1 - \frac{\psi^2}{D^2}\right)(n_1^2 - n_2^2)}\,, \qquad [4a]$$

which for small index differences (i.e., $n_1 - n_2 \ll n_1$) becomes

$$N \cong n_2 + \left(1 - \frac{\psi^2}{D^2}\right)(n_1 - n_2). \qquad [4b]$$

For a laser, the presence of gain in the active layer introduces changes in the imaginary part of the dielectric constant;[15] however, for the transverse direction, we shall neglect the gain contribution to the bulk index of the active layer, since even the largest estimates for that contribution[15,16] are much smaller than $\Delta n = n_1 - n_2$ of a practical device.

3. Approximations for the Guided Mode Propagation

As seen from the previous section, ψ is the crucial parameter in determining the mode propagation in the guide. For this reason we first concentrate on finding a simple yet suitable approximation for ψ. Near the cut-off value (in this case $D = 0$) we use the property of the cosine function of being very well approximated over a relatively wide range by the first two terms of its power series expansion. For instance in approximating $\cos\theta$ by $1 - (\theta^2/2)$ over the range $0 < \theta < \pi/4$ the relative error introduced is at most 2.2%. With this approximation Eq. [2c] becomes

$$D = \frac{\psi}{\cos\left(\frac{\psi}{2}\right)} \simeq \frac{\psi}{1 - \frac{\psi^2}{8}},$$

with the solution for ψ:

$$\psi = 4\frac{\sqrt{1+(D^2/2)}-1}{D}; \qquad 0 < D < \pi. \tag{5}$$

By using Eq. [2c] it can be shown that for small errors in computing $\cos\psi/2$ [i.e. $\Delta(\cos\psi/2) = \cos\psi/2 - (1-(\psi^2/8)) \ll \cos\psi/2$] the relative error for ψ is

$$\frac{\Delta\psi}{\psi} = \frac{1}{1+(D^2/2)} \frac{\Delta\left(\cos\frac{\psi}{2}\right)}{\cos\frac{\psi}{2}} \tag{6}$$

Thus the error introduced by using $\cos\theta \simeq 1-(\theta^2/2)$ is further reduced by the term $1/\sqrt{1+(D^2/2)}$. We find that ψ can be approximated by Eq. [5] within 2% for D values up to π (the cut-off value for the first order mode). For instance, in an (AlGa)As DH guide with $\Delta n = 0.22$ and $\lambda = 0.9\ \mu$m, the case $D = \pi$ corresponds to $d = 0.36\ \mu$m. In general all regions of practical interest in cw diode lasers are within the $0 < D < \pi$ range.[1,2] Although for $D = \pi$ the first order transverse mode could be excited, the fundamental mode is the only one that is observed to lase, most probably due to the difference in mode facet reflectivity.[1] Lasing in the fundamental transverse mode was found to occur up to values of D between 5 and 7 (e.g., up to $d = 0.6$–$0.7\ \mu$m for (AlGa)As lasers with $\Delta n = 0.22$ and $\lambda = 0.9\ \mu$m[1]). For these reasons we also seek approximations for ψ in the $\pi < D < 7$ range. We start far from cut-off (i.e., $\psi = \pi$). For $\psi = \pi - \xi$, we obtain

$$D = \frac{\pi-\xi}{\cos\left(\frac{\pi}{2}-\frac{\xi}{2}\right)} = \frac{\pi-\xi}{\sin\frac{\xi}{2}} \cong \frac{\pi-\xi}{\frac{\xi}{2}} = \frac{2\psi}{\pi-\psi}. \tag{7}$$

As the D value is reduced from ∞ to π the error for the approximation $\sin(\xi/2) = \xi/2$ can be as high as 7%. However, just as in the near-cut-off case, it can be shown that the actual error in computing ψ from Eq. [2c] is less, since

$$\frac{\Delta\psi}{\psi} = \frac{2}{2+D} \frac{\Delta\left(\sin\frac{\xi}{2}\right)}{\sin\frac{\xi}{2}}. \tag{8}$$

From Eq. [7], the expression for the ψ approximation far from cut-off is

$$\psi = \frac{\pi D}{2+D}, \qquad \pi < D < \infty \tag{9}$$

with a maximum error of 2.7% at $D = \pi$. By using different methods, Reinhart et al[17] as well as Marcuse[5] have obtained virtually the same expression for the far-from-cut-off approximation. The ψ versus D plot ($0 < D < 7$) together with the two approximations, are shown in Fig. 2a. The ψ approximation formulae (i.e., Eqs. [5] and [9]) are listed in Table 1, which is a summary of the approximations used for all of the near- and far-field TE_0 mode parameters studied here, together with a previously reported[9] analytical approximation for the TE_0 radiation confinement factor, Γ_0.[17–20]

With the help of the ψ approximations several parameters describing the mode propagation can be accurately determined. Figs. 2b–2d show the variation of three such parameters: the normalized peak field intensity in the guide, E^2_{0max}, the effective waveguide thickness d_{eff}, and the effective waveguide index N. For these calculations, $Al_xGa_{1-x}As$ structures with $\Delta n = 0.1$, 0.22, and 0.34 and $n_1 = 3.6$ are considered.

The normalized field intensity in the guide can be used in calculating the peak field intensity at the facet[1,21]

$$E^2_{max,facet} \simeq E^2_0 \frac{\eta_0 P_0}{n_1(1-R)} 10^5 \left(\frac{\text{kV}}{\text{cm}}\right)^2$$

$$= \frac{\eta_0}{n_1(1-R)} \left(\frac{2P_0}{d_{eff}}\right) 10^5 \left(\frac{\text{kV}}{\text{cm}}\right)^2 \qquad [10]$$

where P_0 is the average power emitted per unit length expressed in $mW/\mu m$, $\eta_0 = 120\pi$ is the vacuum wave impedance, and R is the power reflection coefficient. It is interesting to notice from the last term in Eq. [10] that for the maximum field intensity at the facet, the power density per unit area is twice the average value usually considered for a laser (i.e., P_0/d_{eff}). One can use Eq. [10] to estimate laser degradation and/or catastrophic facet damage levels.[1] Fig. 2b shows that for all structures E^2_{0max} has a maximum around $D = 1.74$, which thus should be the worst place for high power laser operation (e.g., for a structure with $\Delta n = 0.22$, the case $D = 1.74$ corresponds to $d = 0.2$ μm). This maximum in field intensity also corresponds to a 60% ratio of the energy propagating in the active layer versus the total mode energy (i.e., $\Gamma_0 \cong 0.6$). The approximations shown in Fig. 2b for E^2_{0max} have a maximum error of 0.7%. Very similar accuracy is obtained in calculating d_{eff}, the effective waveguide width (Fig. 2c). As expected, the minima of the d_{eff} curves occur for $D = 1.74$. The effective width is an important parameter when energy exchange is considered[14], and also is a measure of the degree of light confinement to the active layer.

The effective index N is shown in Fig. 2d. Maximum approximation errors (i.e., at $D = \pi$) amount to only 3×10^{-3} for $\Delta n = 0.22$. In the expression for N, the factor $1 - \psi^2/D^2$ (sometimes called the normalized

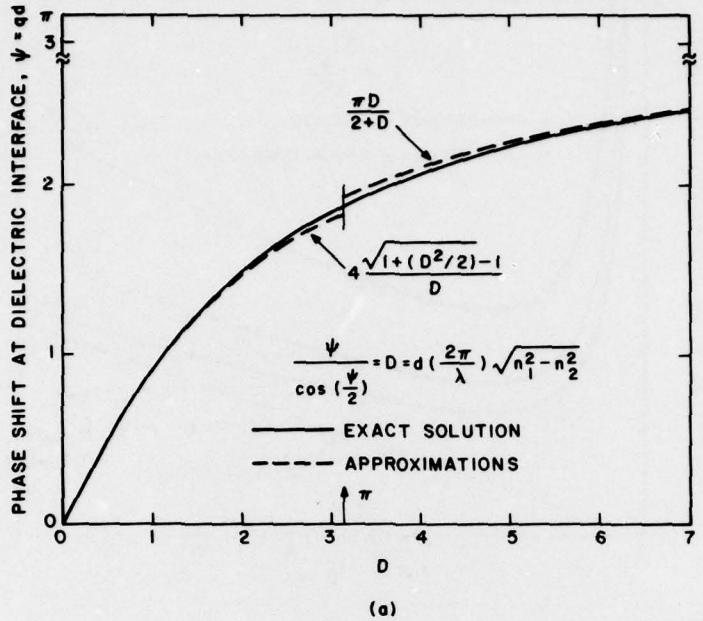

(a)

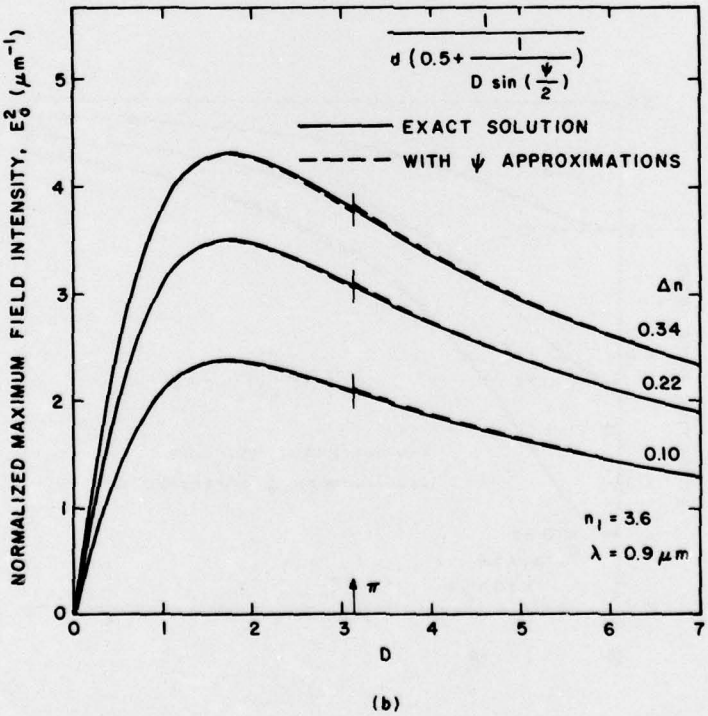

(b)

Fig. 2—The variation with respect to the normalized waveguide thickness $D \equiv (2\pi/\lambda)d\sqrt{n_1^2 - n_2^2}$ of the exact solutions (solid curves) and approximations (dashed curves) for: (a) ψ, the mode phase shift at the dielectric interface upon total internal reflection; (b) $E^2_{0(max)}$, the maximum field intensity in the guide for the case when the fields have been normalized to unity (Eq. [3a]); (continued)

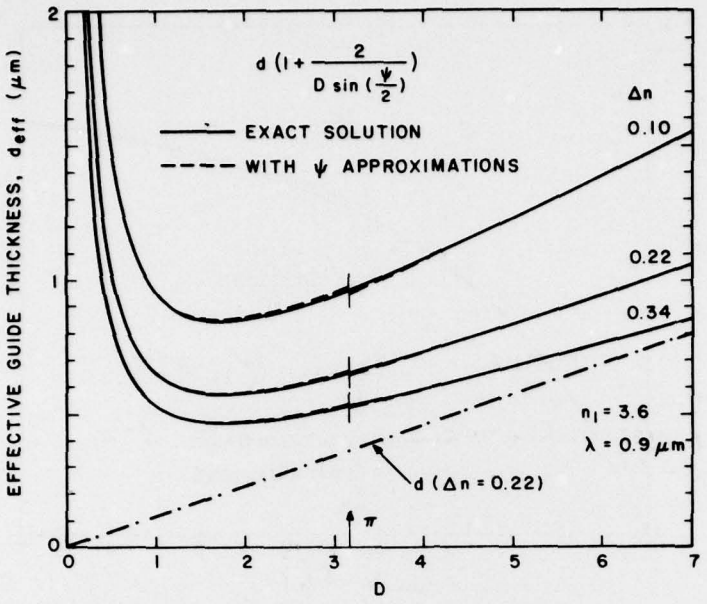

(c)

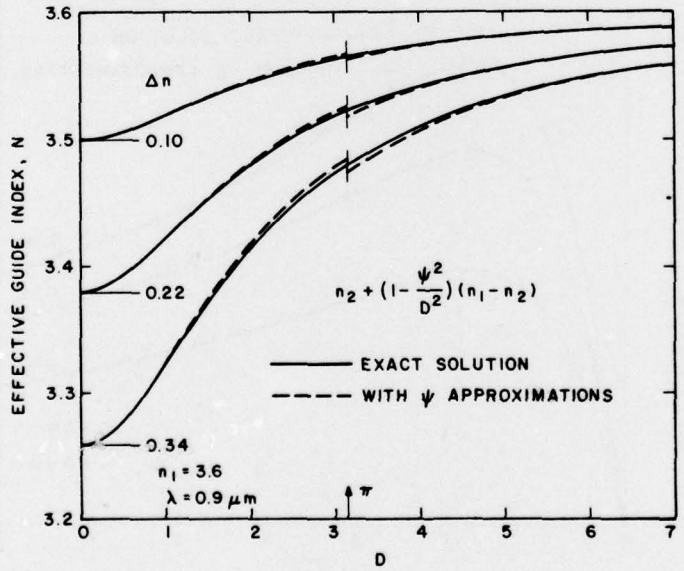

(d)

Fig. 2 (continued) (c) d_{eff}, the effective waveguide thickness (for comparison we plot d for $\Delta n = 0.22$); (d) N, the effective waveguide index. The parameters shown in (b) – (d) are plotted for $Al_{1-x}Ga_xAs$ DH structures with $n_1 = 3.6$, $\lambda = 0.9\ \mu m$, and for $\Delta n = 0.1$, 0.22, and 0.34. The extrema of the E_0^2 curves (i.e., maxima) and d_{eff} curves (i.e., minima) occur at $D = 1.74$.

guide index, b[14]) can also be written as $\sin^2(\psi/2)$, but only for the TE_0 mode (i.e., $b \cong (N - n_2)/(n_1 - n_2) = \sin^2(\psi/2)$). The formulation of b in terms of ψ only, allows a simple expression for the wavepacket longitudinal shift upon total internal reflection at the dielectric interface:[14]

$$2z_s = \frac{d\psi}{d\beta} = \frac{\lambda}{\pi \Delta n \sin\psi},$$

i.e., the Goos-Hänchen shift. Also, it can be easily shown that as $D \to 0$, b approaches asymptotically the value $D^2/4$, and consequently $(\Gamma_0/2)$,[9] rather than Γ_0.[16] The effective index is a very useful concept when considering lateral light confinement in structures of varying active layer thickness[11,22,23,42] as well as in buried lateral guides.[24,25]

The approximations presented above refer only to TE_0 modes of symmetric guides. For the TM_0 mode of symmetric guides the difference occurs in the characteristic equation [2c]. Using the expressions of Anderson[4] it can be shown that the characteristic equation is

$$\frac{\psi}{\cos\frac{\psi}{2}} = D\left(\frac{n_1}{n_2}\right)^2 \Big/ \sqrt{\left(\frac{n_2}{n_1}\right)^4 + \left(1 - \frac{n_2}{n_1}\right)^4 \cos^2\left(\frac{\psi}{2}\right)} \qquad [11]$$

Approximation formulae for ψ can be easily found by using the same methods as for the TE_0 mode. The errors thus introduced have values very similar to the ones for the TE_0 mode (i.e., <2%). Table 2 summarizes the near-field approximations for the TM_0 mode of symmetric DH structures. We include in Table 2 an approximate formula for the TM_0 mode radiation confinement factor, $\Gamma_{0(TM)}$, which was obtained in a similar manner as the $\Gamma_{0(TE)}$ analytical approximation.[9] The expression is found to agree fairly well (within 10%) with numerically calculated curves by Hakki and Paoli.[19]

For asymmetric guides ($n_3 > n_2$) an asymmetry factor $\eta = (n_1^2 - n_2^2)/(n_1^2 - n_3^2)$ is used in the characteristic mode equation [4]. Table 3 gives the characteristic equations for TE_0 and TM_0 modes and an analytical approximation for Γ_0 of asymmetric guide TE_0 modes (the same method as in Ref. [9] was used). Again explicit (approximate) solutions for ψ over the intervals $0 < D < \pi$ and $D > \pi$ could be obtained and, thus, one could approximate various near-field parameters.[5,14] However, we limit ourselves in this paper to symmetric guides ($\eta = 1$), since the approximations for the asymmetric DH case would be considerably more complex, and because few practical DH lasers are of the asymmetric type. These are treated in detail in Ref. [1].

In an article concerning light propagation in symmetric multimode guides,[7] Lotspeich uses similar mathematical approximations for ψ, but

Table 1—TE_0 Mode in Symmetric DH Structures

Parameter	Definition	Approximation	Range of $D \equiv \frac{2\pi}{\lambda} d\sqrt{n_1^2 - n_2^2}$
ψ	$\psi = D \cos\left(\frac{\psi}{2}\right)$	$4(\sqrt{1 + (D^2/2)} - 1)/D$	$0 < D < \pi$
	Characteristic equation	$\pi D/(2 + D)$	$\pi < D < \infty$
ψ'	$D \sin\left(\frac{\psi}{2}\right)$	Use formulae for ψ over same D intervals	
d_{eff}	$d\left(1 + 2/D \sin\left(\frac{\psi}{2}\right)\right)$		
$N_{(eff)}$	$n_2 + \left(1 - \frac{\psi^2}{D^2}\right)(n_1 - n_2)$		
E_0^2	$1/d\left(0.5 + 1/D \sin\left(\frac{\psi}{2}\right)\right)$		
$E_y(x)$	$E_0 \cos\left(\frac{\psi}{d}x\right)$, $\quad \lvert x\rvert < \frac{d}{2}$ $E_0 \cos\left(\frac{\psi}{2}\right) \exp\left\{-\frac{\psi'}{d}\left(\lvert x\rvert - \frac{d}{2}\right)\right\}$, $\quad \lvert x\rvert > \frac{d}{2}$	$\sqrt{\frac{\sqrt{2}}{w\sqrt{\pi}}}\, e^{-x^2/w^2}$ $w = d(0.31 + 2.1/D^{3/2} + 4/D^6)$	$1.8 < D < 6$

Γ_0	$\int_{-d/2}^{+d/2} E_y^2(x)dx$	$D^2/(2+D^2)$	$0 < D < \infty$
$\theta_\perp$	$\frac{I(\theta_\perp/2)}{I(0)} = \frac{1}{2}$	$2\tan^{-1}(\lambda\, 0.59/\pi w_0)$ $w_0 = d(0.31 + 3.15/D^{3/2} + 2/D^6)$	$1.5 < D < 6$ $\frac{\Delta n}{n} < 10\%$
		$0.65\, D\sqrt{n_1^2 - n_2^2}/(1 + 0.086\kappa D^2)$ $\kappa = [2.52\sqrt{n_1^2 - n_2^2}/\tan^{-1}(0.36\sqrt{n_1^2 - n_2^2})] - 5.17$	$0 < D < 1.5$
$\frac{I(\theta)}{I(0)}$	$\frac{\cos^2\theta \left\lvert \int_{-\infty}^{+\infty} E_y(x')e^{-2\pi jx'\sin\theta/\lambda}dx \right\rvert^2}{\left\lvert \int_{-\infty}^{\infty} E_y(x')dx \right\rvert^2}$	$\exp\left[-\frac{0.69\theta^2}{(\theta_{1/2})^2}\right]$; $\theta_{1/2} = \frac{\theta_\perp}{2}$	$1.5 < D < 6$ $\frac{\Delta n}{n} < 10\%$
		$\cos^2\theta[\psi'\psi^2(2\psi' - A^2)/2(\psi^2 - A^2)(\psi'^2 + A^2)]^2$ $A = D\sin\theta/\sqrt{n_1^2 - n_2^2}$	$0 < D < 1.5$ $\theta_\perp < 40°$

ψ = product of the transverse progagation constant q and the active layer thickness d (also the TE_0 mode phase shift at the dielectric interface upon total internal reflection);

ψ' = product of the exponential decay constant p and the active layer thickness d;

d_{eff} = effective waveguide thickness; N = effective waveguide index; E_0^2 = maximum field intensity in the guide for the case when the fields are normalized to unity (Eq. [3a]); $E_y(x)$ = optical field distribution in the guide;

Γ_0 = radiation confinement factor[9]; $\theta_\perp$ = half-power beamwidth of the laser radiation pattern; $I(\theta)/I(0)$ = relative far-field distribution of the beam intensity.

Table 2—TM_0 Mode in Symmetric DH Structures (Near-Field)

Parameter	Definition; $m = n_2/n_1$	Approximation	Range of $D \equiv \frac{2\pi}{\lambda} d\sqrt{n_1^2 - n_2^2}$
ψ	$\psi = D \Big/ \sqrt{1 + m^4 \tan^2\left(\frac{\psi}{2}\right)}$ Characteristic equation	$4\sqrt{\frac{2 + (D^2/2) - 2\sqrt{1 + (D^2/2)(2m^4 - 1)}}{D^2 + 16\,(1 - m^4)}}$	$0 < D < \pi$
		$\pi D/(2m + D)$	$\pi < D < \infty$
ψ'	$\sqrt{D^2 - \psi^2}$	Use formulae for ψ over same D intervals	
d_{eff}	$d(1 + 2m^2D^2/[\psi'(D^2 - \psi^2(1 - m^4))])$		
H_0^2	$2/d_{eff}$		
$N_{(eff)}$	$n_2 + \left(1 - \frac{\psi^2}{D^2}\right)(n_1 - n_2)$		
Γ_0	$\int_{-d/2}^{d/2} E^2(x)dx$	$m^4D^2/(2 + m^4D^2)$	$0 < D < \infty$

Table 3—Asymmetric DH Structures

Mode	Characteristic Equation
TE_0	$\psi^2 = \sqrt{(D^2 - \psi^2)(\eta D^2 - \psi^2)} + \sqrt{\eta}\, D^2 \cos\psi$
TM_0	$\psi = \tan^{-1} \frac{n_1^2}{n_2^2} \frac{\sqrt{D^2 - \psi^2}}{\psi} + \tan^{-1} \frac{n_1^2}{n_3^2} \frac{\sqrt{\eta D^2 - \psi^2}}{\psi}$
Parameter	Approximation; $1 < \eta < \infty$
$\Gamma_{0_{TE}}$	$\frac{\Gamma_0}{1 + \Gamma_0'}$; $\quad \Gamma_0' = \frac{2\sqrt{\eta}}{1 + \sqrt{\eta}} D(D - \tan^{-1}\sqrt{\eta - 1}) \times \left[1 + \frac{1}{\sqrt{\eta^2\, 1 + (\eta - 1)/(D - \tan^{-1}\sqrt{\eta - 1})^2}}\right]^{-1}$

Definitions:

$$D \equiv \frac{2\pi}{\lambda} d\sqrt{n_1^2 - n_2^2};\ \eta = \frac{n_1^2 - n_2^2}{n_1^2 - n_3^2};\ n_3 > n_2$$

$$\Gamma_{0_{TE}} = \int_{-d/2}^{d/2} E_y^2(x)dx$$

only over limited ranges, since his purpose is to find ψ asymptotes. The asymptotes are then used in a linear combination with variable coefficients chosen to provide a good ψ approximation. While very accurate, the resulting ψ formula is rather complicated. We believe that our relatively simple approximations for ψ, over intervals of D, are more than adequate in precisely describing the behavior of fundamental transverse modes in symmetric guides.

4. Approximations of the Mode Near-Field Distribution

The electric field variation in the transverse direction (Eq. [1]) as well as the peak field amplitude (Eq. [3]) depend directly on ψ, the phase shift at the dielectric interface. Since, as shown in the previous section, ψ can be approximated very well over its whole range ($0 \leq \psi \leq \pi$), a precise determination of the mode field distribution in the active layer as well as in the cladding layers is readily obtainable. However, in many cases (e.g. scattering loss calculations, radiation loss calculations, etc.) the description of the near-field by a single function would greatly simplify the analysis. One such single-function field description can be obtained by using the Epstein-layer model[26], but the expressions that have to be used are very complicated. In a recent paper[27] Marcuse presents Gaussian field approximations for the fundamental modes of graded-index and step-index weakly guiding fibers ($\Delta n \ll n_1$). We also use a Gaussian approximation in trying to describe the field distribution in symmetric double-heterostructure slab waveguides. In Sections 6 and 8, the Gaussian approximation concept is extended to the transverse mode far-field pattern. Just as in the case of fibers[27] the Gaussian approximation for the fundamental mode is good only over a certain range

of D, the normalized guide thickness. For small D's the mode lies mostly outside the active layer and thus it assumes a double-exponential-like shape. At the other extreme, when the mode is mostly confined to the guide, (i.e., large D's) the field distribution will be cosine-like. We fit a Gaussian to the field distribution in the intermediate region[28] (i.e. a field shape made of both a cosine curve and exponential curves).

A Gaussian field distribution is described by the following expression:

$$E_G(x,z) = \sqrt{\frac{\sqrt{2}}{w\sqrt{\pi}}} \exp\left\{-\frac{x^2}{w^2} - i\beta z\right\}; \qquad -\infty < x < \infty, \quad [12]$$

where w is the Gaussian beam width parameter, defined as the value of x at which the field amplitude is $1/e$ of the peak amplitude. The peak amplitude was determined by normalizing the fields to unity. The Gaussian field distribution Eq. [12] is to be compared to the TE_0 mode field distribution $E_y(x,z)$ as defined by Eqs. [1] and [3].

The ideal approach for the Gaussian fit is to find the beam width parameter w such as to maximize the variational integral[27]

$$\int_{-\infty}^{\infty} E_G(x)E_y(x)dx. \qquad [13]$$

However, this requires extensive numerical calculations. We chose to first determine the asymptotic value of w/d as $d \to \infty$ and then find the rest of the function w/d (D) by trial and error. As d tends to ∞, $d_{eff} \to d$ and $\psi \to \infty$; this gives for $E_y(x)$ the form $\sqrt{2}/\sqrt{d}\cos(\pi x/d)$. Thus, we have to maximize the expression:

$$\frac{\sqrt{2}}{\sqrt{d}}\sqrt{\frac{\sqrt{2}}{w\sqrt{\pi}}}\int_{-\infty}^{\infty}\cos\left(\frac{\pi x}{d}\right)\exp\{-x^2/w^2\}dx$$
$$= \sqrt{\frac{2\sqrt{2\pi}w}{d}}\exp\left\{-\frac{\pi^2 w^2}{4d^2}\right\}. \qquad [14]$$

Assuming $w = \alpha d$, it can be shown that Eq. [14] assumes a maximum for $\alpha = 1/\pi \simeq 0.31$. Therefore $w/d = 0.31 + f(D)$, where $f(D) \to 0$ as $D \to \infty$. To find $f(D)$ we use as a trial function $f(D) = (\beta/D^{3/2}) + (\gamma/D^6)$, which is similar to the function empirically determined by Marcuse for fibers. By trial and error, and also by using the correlation between the field in the guide and a Gaussian approximation for the far-field (see Section 7), we find a best fit for

$$\frac{w}{d} = 0.31 + \frac{2.1}{D^{3/2}} + \frac{4}{D^6}; \qquad 1.8 < D < 6. \qquad [15]$$

Figs. 3a, b, c show comparisons of Gaussian field distributions versus the exact solutions for $D = 2$, 3, and 4 and $\Delta n = 0.22$ ($n_1 = 3.6$; $\lambda = 0.9$

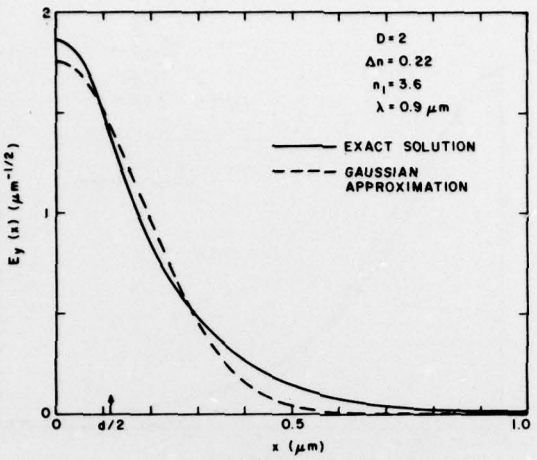

(a)

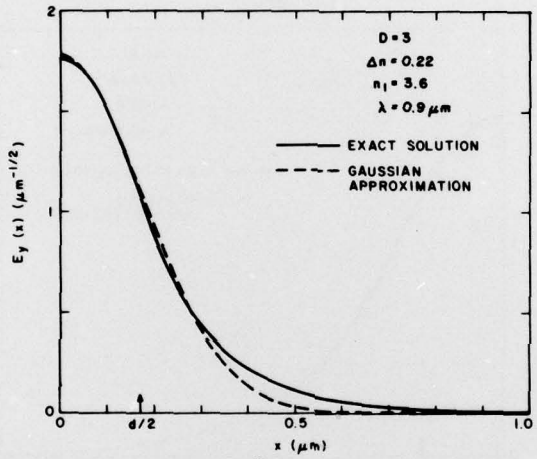

(b)

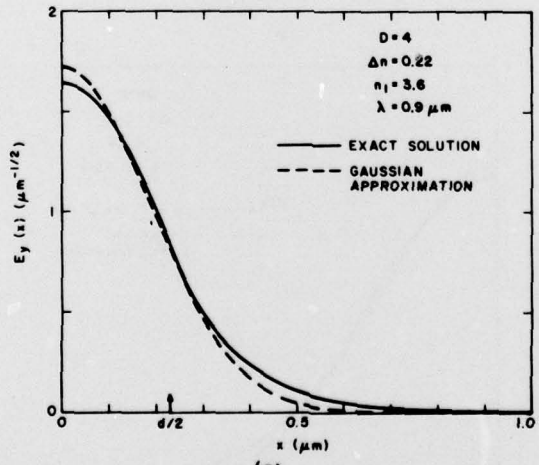

(c)

Fig. 3—Comparison of near-field distribution profiles (solid curves) $E_y(x)$ (Eqs. [1] and [3b]) versus the Gaussian approximation (dashed curves) $E_G = \sqrt{\sqrt{2}/w\sqrt{\pi}}\exp(-x^2/w^2)$ with $w = d(0.31 + 2.1/D^{3/2} + 4/D^6)$, for: (a) $D = 2$, $\Delta n = 0.22$; (b) $D = 3$, $\Delta n = 0.22$; (c) $D = 4$, $\Delta n = 0.22$. All graphs are plotted for structures with $n_1 = 3.6$ and $\lambda = 0.9$ μm.

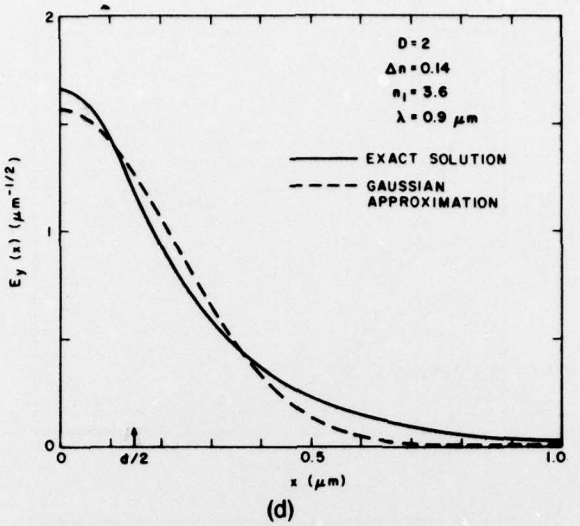

(d)

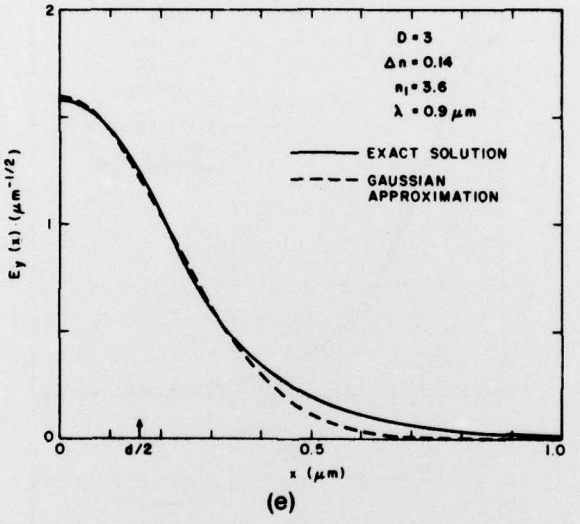

(e)

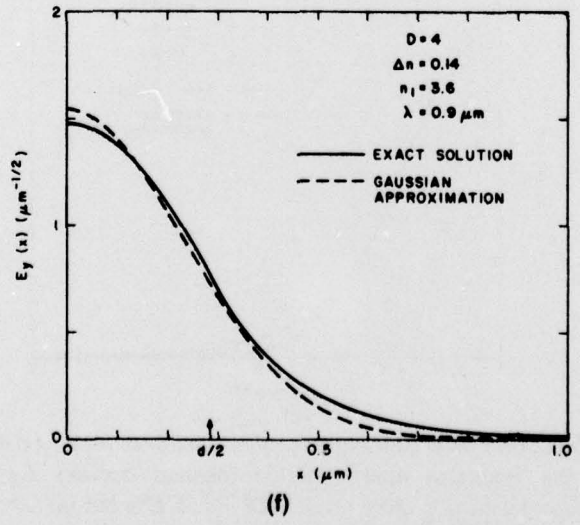

(f)

Fig. 3 (continued)—(d) $D = 2$, $\Delta n = 0.14$; (e) $D = 3$, $\Delta n = 0.14$; (f) $D = 4$, $\Delta n = 0.14$.

μm). The curves agree very well for D values around 3 and 4. Figs. 3d, e, f show similar comparisons for the case $\Delta n = 0.14$. The fit is still very good. As mentioned previously, the field distribution in the guide is almost identical to the field distribution on the facet, and thus Eqs. [12] and [15] give a Gaussian approximation for the near-field as well.

Reinhart et al[17] have shown that a Gaussian description of the near-field is useful when computing mode reflection coefficients in DH structures with $D \geq 3$. The authors claim as an upper limit for an acceptable Gaussian fit the condition $\psi < 2.4$, which corresponds to $D = 6.6$ and thus agrees with our findings. For $D < 2$ (e.g., $d < 0.25$ μm when $\Delta n = 0.22$, $n_1 = 3.6$, and $\lambda = 0.9$ μm) the Gaussian near-field approximation will be increasingly poor and thus cannot be used for predicting modal facet reflection coefficients.[29] In a recent article, Utaka et al[30] use an expression similar to Eq. [15] for a near-field Gaussian approximation, which appears to be good over the interval $\pi < D < 6$.

5. Mode Far-Field Intensity Distribution

The lasing mode far-field intensity distribution is the laser radiation pattern at large distance from the mirror facet ($r \gg \lambda$). For the transverse mode case, we are interested in the electric field distribution in the plane perpendicular to the junction as a function of θ, the angle with respect to the normal to the laser facet. When θ assumes small values (i.e., $\cos\theta \simeq 1$), the far-field angular field distribution is obtained as the Fourier transform of the near-field distribution (i.e., the aperture field)[1,18,28]

$$G'\left(\frac{\sin\theta}{\lambda}\right) = \int_{-\infty}^{\infty} E_y'(x) \exp\left[-2\pi j x \left(\frac{\sin\theta}{\lambda}\right)\right] dx, \qquad [16]$$

where $E_y'(x)$ stands for the field distribution at the laser facet. The far-field dependence on r, the distance from the observation point to the center of the near-field distribution (i.e. $[\exp\{-j(2\pi/\lambda)r\}]/r$), is omitted since we are interested only in the field variation with the angle θ at fixed r. For large angles however, an obliquity factor $g(\theta)$ must be used.[28,29,31–33] Then the correct expression for the far-field angular field distribution $E(\theta)$ is

$$E(\theta) = g(\theta)G'\left(\frac{\sin\theta}{\lambda}\right). \qquad [17]$$

In order to calculate $E(\theta)$ some simplifications are made. First one computes the Fourier transform of the field inside the guide, $G(\sin\theta/\lambda)$,[1,18,28] since, as mentioned previously, $E_y(x)$ is only slightly different from the field distribution on the facet $E_y'(x)$. Then, for the obliquity factor, the function $\cos\theta$ is used, which has been shown theoretically[31]

as well as experimentally[1,28] to be a very good approximation of $g(\theta)$. Thus the far-field intensity pattern $I(\theta)$ is given by

$$I(\theta) = |E(\theta)|^2 = \cos^2\theta \left| G\left(\frac{\sin\theta}{\lambda}\right)\right|^2. \quad [18]$$

While this expression is found to very accurately predict experimental far-field patterns,[1,28,32] its computation is difficult since $G(\sin\theta/\lambda)$ is a rather complicated expression. Furthermore, in order to find the beamwidth $\theta_\perp = 2\theta_{1/2}$ (fwhp) the transcendental equation $[I(\theta_{1/2})/I(0)] = 1/2$ has to be solved. Dumke[8] has found an approximation formula for $\theta_\perp$ for very thin active layers, by combining the asymptotes of $\theta_\perp$ as $d \to 0$ and as $d \to \infty$. However, as will be shown in the Section 7, Dumke's formula is a reasonably good approximation only over a very limited parameter range ($d < 0.1$ μm and $\Delta n < 0.22$). In the next section we use a Gaussian approximation of the far-field pattern over the range $1.5 < D < 6$ in order to find very accurate expressions for $\theta_\perp$ over wide parameters ranges ($0 < D < 6$ and $\Delta n/n \leq 10\%$). Furthermore we also can predict fairly well the far-field intensity patterns.

6. Beamwidth Gaussian Approximation ($1.5 < D < 6$)

It was shown in Section 4 that the field distribution in the waveguide can be described quite accurately by a Gaussian field distribution over the D range 1.8 to 6. Then, it should not be surprising to find a Gaussian distribution in the far-field as well. Furthermore the obliquity factor can be approximated by a Gaussian-like function[32]

$$\cos\theta \simeq \exp\left\{-\frac{\theta^2}{2}\right\} \quad [19]$$

within 2% for $0 < \theta < 40°$.

The angular beam spread for a fundamental Gaussian beam has the form[34,35]:

$$\theta_{beam} = \tan^{-1}\left(\frac{\lambda}{\pi w_0}\right), \quad [20]$$

where w_0 is the beam minimum waist and θ is the angle measured from the z axis. The parameter θ_{beam} is the angle at $1/e$ of the far-field angular field distribution. In order to obtain $\theta_{1/2}$ (the angle at 1/2 of the far-field intensity distribution), a factor of $0.59 = \sqrt{(\ln 2)/2}$ should be added in Eq. [20],

$$\theta_{1/2} = \tan^{-1}\left(\frac{\lambda 0.59}{\pi w_0}\right). \quad [21]$$

To find w_0 by starting in the near-field is not an easy task since, as

mentioned above, an obliquity factor has to be considered for the far-field distribution. For this reason we chose to find w_0 by fitting the expression $\theta_\perp = 2\theta_{1/2} = 2\tan^{-1}(\lambda 0.59/\pi w_0)$ to numerically calculated beamwidth curves by Butler and Kressel.[1] From the Gaussian fit of the near-field distribution, we know that w_0 should have the form $w_0/d = 0.31 + \beta/D^{3/2} + \gamma/D^6$. The best fit to numerical computed $\theta_\perp$ curves is found for $\beta = 3.15$ and $\gamma = 2$ over the range $1.5 < D < 6$. Thus we obtain for the beamwidth the approximation formula:

$$\theta_\perp = 2\tan^{-1}\left(\frac{\lambda 0.59}{\pi w_0}\right), \qquad [22]$$

with

$$w_0 = d[0.31 + (3.15/D^{3/2}) + (2/D^6)] \qquad \text{for } 1.5 < D < 6.$$

The actual beam minimum waist is not w_0 but w, the Gaussian parameter of the near-field profile (see Eq. [12]). The difference is due to the obliquity factor $g(\theta)$. It can be easily checked, via the far-field intensity pattern Eqs. [18] and [24], that Eq. [22] contains the contributions of both the near-field Gaussian approximation, Eq. [12], as well as the obliquity factor, $\cos\theta$. Fig. 4 shows a comparison of the Gaussian approximation ($D > 1.5$) versus numerical data by Butler and Kressel for various $\Delta n = n_1 - n_2$ values with $n_1 = 3.6$ and $\lambda = 0.9\,\mu$m. The agreement is very good (within 2%) for Δn values between 0.14 and 0.26, which also is the region of most interest in $Al_xGa_{1-x}As$ lasers ($\Delta n \simeq 0.65\,\Delta x$)[1]. It must be stressed that the numerical calculations by Butler and Kressel agree extremely well with experimental data of various workers.[18,32,36] The curve $D = \pi$ in Fig. 4 signifies the cutoff for excitation of the first order mode and also happens to be the locus of the $\theta_\perp$ curves maxima for given Δn. As mentioned previously, although the first order mode can be excited, due to modal gain considerations it does not lase until D has values somewhere between 5 and 6 (e.g., 0.6–0.7 μm for $\Delta n = 0.18$).[1,2] Thus the $\theta_\perp$ curves have to be considered up to those D values. From Fig. 4 it can be seen that for $1.5 < D < 5$ the Gaussian approximation is good within 4% for $0.06 < \Delta n < 0.34$. Yet as $D \to \infty$, Eq. [22] gives $\theta_\perp \to 1.2\,\lambda/d$ which is the expected behavior in the limit that the near-field distribution becomes a cosine function.[8] For large Δn values (e.g., $\Delta n \geq 0.42$), Eq. [22] fails to give a good approximation for $\theta_\perp$, which we expect since both the obliquity factor and the near-field distribution[27] tend to diverge from a Gaussian-like shape. Since the $\theta_\perp$ formula applies for any type of symmetric double-heterojunction (e.g., GaAs-AlGaAs, InP-InGaAsP), we conclude that the Gaussian approximation for the fundamental mode beamwidth is accurate within 4% for $1.5 < D < 5$ and for $\Delta n/n < 10\%$.

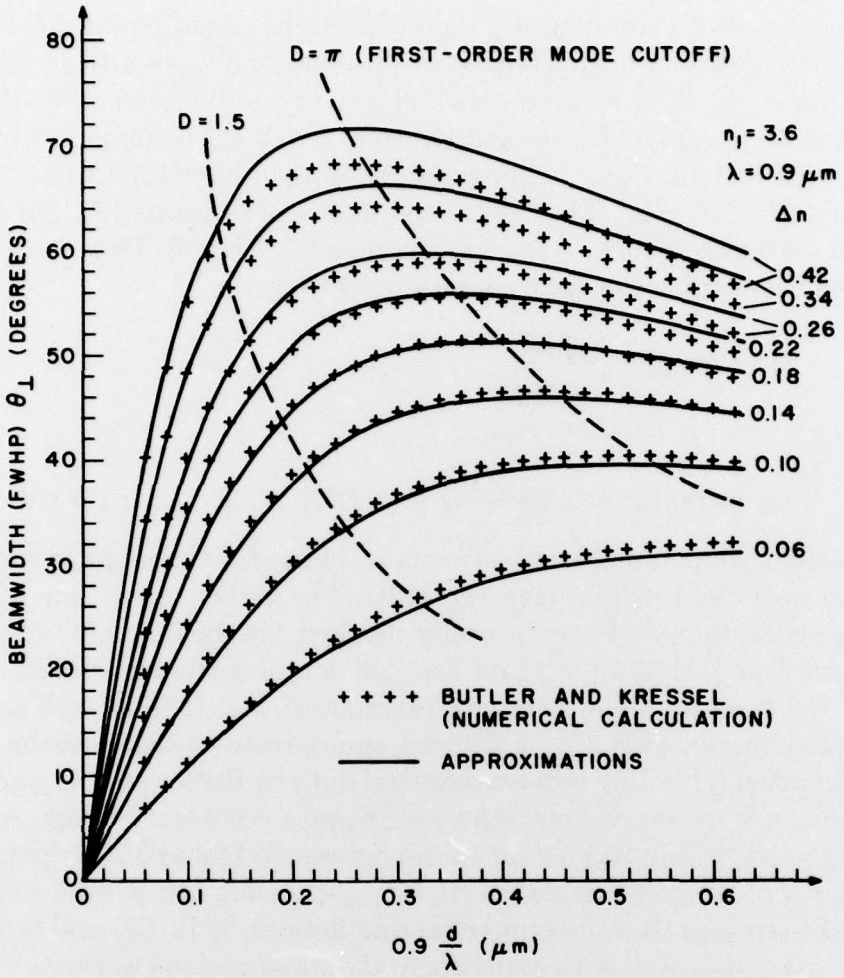

Fig. 4—The beamwidth $\theta_\perp$ (full width at half power) for the laser radiation pattern, in the plane perpendicular to the junction, as a function of a wavelength normalized active layer thickness, and for different index steps Δn (0.06 to 0.42). The crosses correspond to numerically calculated points by Butler and Kressel.[1] The solid curves are approximations: an asymptotic approximation for $0 < D < 1.5$ (see Fig. 5) and a Gaussian approximation for $1.5 < D < 6$ (i.e., $\theta_\perp = 2 \tan^{-1}[\lambda 0.59/\pi w_0]$ with $w_0 = d[0.31 + 3.15/D^{3/2} + 2/D^6]$, where $D = [2\pi/\lambda]d\sqrt{n_1^2 - n_2^2}$).

7. Beamwidth for Thin Active Layers ($0 < D < 1.5$)

For $D < 1.5$, the beamwidth Gaussian approximation Eq. [22] is no longer appropriate. The near-field patterns have double-exponential shapes[28] and become relatively wide, which in turn gives far-field angular distributions of narrow beamwidth and non-Gaussian shapes. In order to approximate the beamwidth we use Dumke's formula[8] with a correction factor κ chosen to match the Gaussian approximation at $D = 1.5$. We thus obtain

$$\theta_\perp \cong \frac{4.09(d/\lambda)(n_1^2 - n_2^2)}{1 + 3.39\kappa(d/\lambda)^2(n_1^2 - n_2^2)}$$

$$= \frac{0.65D\sqrt{n_1^2 - n_2^2}}{1 + 0.086\kappa D^2}; \qquad 0 < D < 1.5 \quad [23]$$

with

$$\kappa = \frac{2.52\sqrt{n_1^2 - n_2^2}}{\tan^{-1}(0.36\sqrt{n_1^2 - n_2^2})} - 5.17.$$

As can be seen from Fig. 4, this approximation is very good. The factor κ varies almost linearly between 1.95 and 2.9 as Δn takes values between 0.06 and 0.6 (e.g., $\kappa = 2.2$ when $\Delta n = 0.18$). For the reader's benefit, we show in Fig. 5 values of $\theta_\perp$ over the very thin active layer region $0 < 0.9\, d/\lambda < 0.2$ μm, and for additional Δn values (0.5 and 0.6). We also extend the approximation Eq. [22] beyond the $D = 1.5$ limit up to $d = 0.2$ μm (for $\Delta n > 0.18$). For comparison, we plot dashed curves[8] corresponding to the case $\kappa = 1$, for two Δn values, 0.22 and 0.6. It appears that Dumke's formula considerably overestimates the beamwidth for $d > 0.1$ μm at $\Delta n = 0.22$ and for $d > 0.05$ μm at $\Delta n = 0.6$. The previously reported[8] relatively good fit of Dumke's formula to beamwidth curves published by Casey et al[18] is thought to arise from the fact that in the latter study the obliquity factor was not considered.[32,35] The $\theta_\perp$ curves of Fig. 5 should prove useful for an estimate of Δn once $\theta_\perp$, d, and λ have been accurately determined experimentally.[1]

8. Far-Field Patterns

We showed in Section 6 that a Gaussian approximation is a very good fit when trying the estimate the laser beamwidth for $D > 1.5$ and $\Delta n/n < 10\%$. We thus expect that for the same ranges of parameter variation, the far-field intensity pattern is very much like a Gaussian curve. Therefore we assume:

$$I(\theta) = \exp\left\{-\frac{0.69\theta^2}{(\theta_{1/2})^2}\right\}; \qquad D > 1.5; \frac{\Delta n}{n} < 10\%, \quad [24]$$

where $\theta_{1/2} = \theta_\perp/2$ is given by Eq. [22] and the factor 0.69 is introduced such that when $\theta = \theta_{1/2}$, $I(\theta)$ drops to half its value at $\theta = 0$. Previously, Lewin[32] also proposed a Gaussian form for the far-field intensity pattern, but he assumed it should work only for small angles and with no restriction on D. In the same article Lewin finds very good agreement between his Gaussian approximation corrected for the obliquity factor, and an experimental far-field pattern of a structure with $D = 1.52$ ($\Delta x = 0.3$, $d = 0.18$, $\lambda = 0.89$ μm). As shown in Figs. 6a and b, we also find good fit to Gaussian curves of experimentally obtained far-field patterns from structures with $D > 1.5$. Thus, Fig. 6a shows an excellent agreement between a Gaussian and the experimental[37] far-field intensity profile of a structure with $D = 3.68$ and $\Delta n = 0.08$ ($\theta_{1/2} = 19°$). For structures

with $\theta_{1/2}$ larger than $\simeq 25°$, there is some disagreement in the curve tails as shown in Fig. 6b (i.e., for a Gaussian versus experimental[33] far-field of $\theta_{1/2} = 25.5°$ obtained from a laser with $D = 2.16$). We believe that this effect is mainly due to the obliquity factor deviation from a Gaussian-like form for $\theta > 40°$. Overall though, down to approximately 25% of the peak

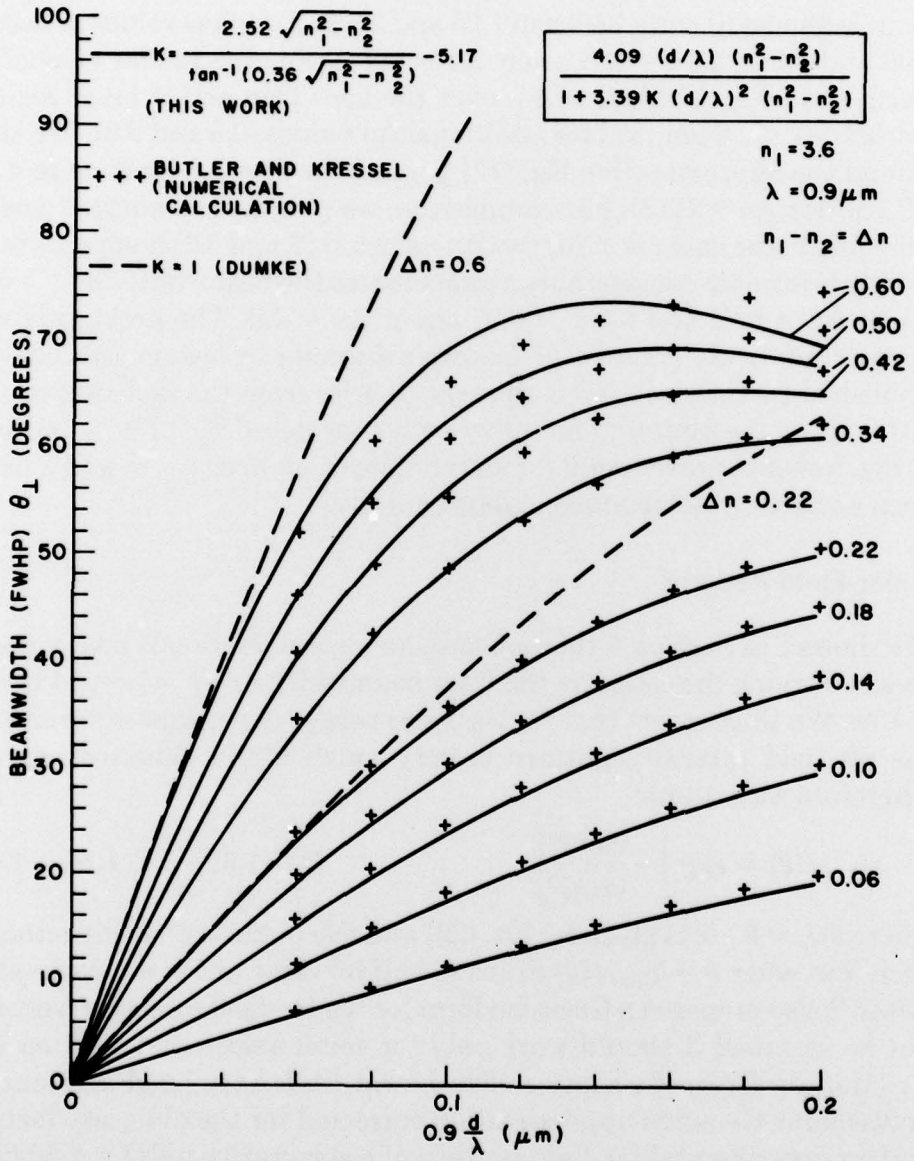

Fig. 5—Laser radiation pattern beamwidth $\theta_\perp$ for thin active layers (i.e., $0 < 0.9d/\lambda < 0.2$ μm). The crosses correspond to Butler and Kressel's numerical calculations,[1] while the solid curves correspond to the approximation formula inserted in the top right corner. The case $\kappa = 1$(Dumke's formula[8]) is represented by dashed curves for $\Delta n = 0.22$ and 0.6. All curves are computed for DH structures with $n_1 = 3.6$ and $\lambda = 0.9$ μm.

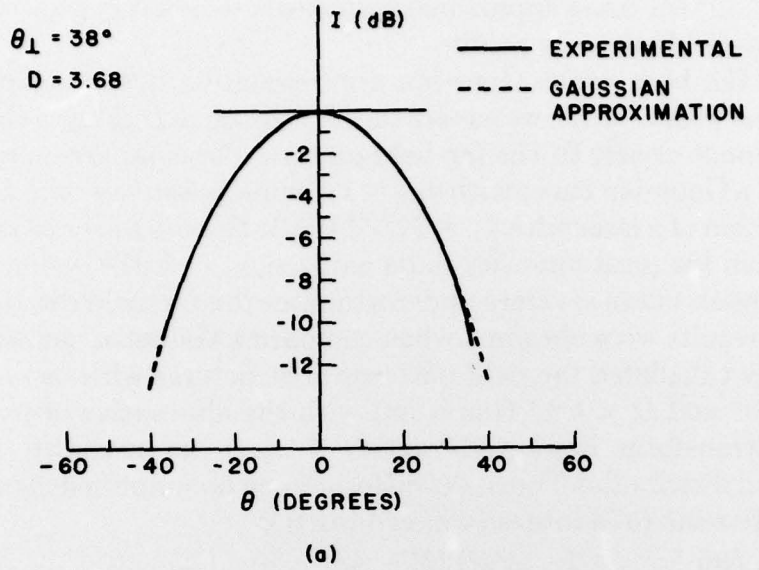

(a)

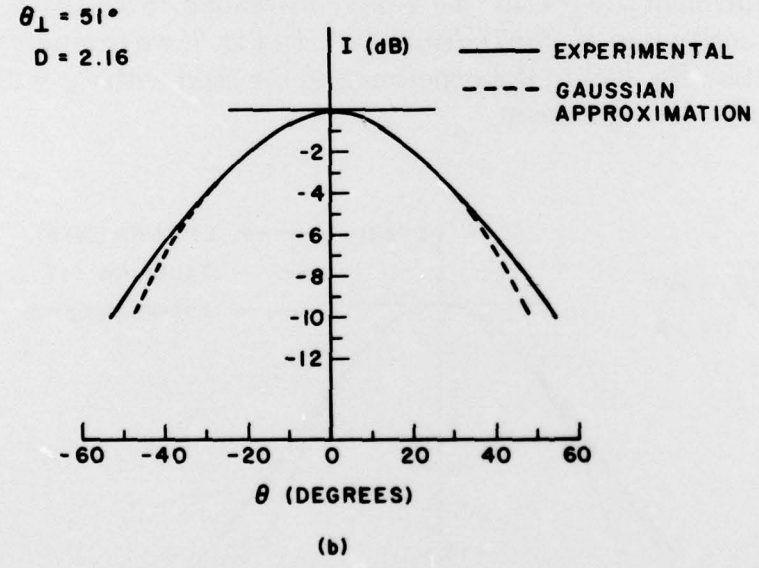

(b)

Fig. 6—Comparison of experimental (solid curves) far-field patterns (from Refs. [37] and [33], respectively) to the Gaussian approximation (dashed curves) $I(\theta)/I(0) = \exp(-0.69\ \theta^2/(\theta_{1/2})^2)$, where $\theta_{1/2} = \theta_\perp/2$ is given by Eq. [22]: (a) $d = 0.7\ \mu$m, $\Delta n = 0.08$; $D = 3.68$, $\theta_\perp = 38°$; (b) $d = 0.25\ \mu$m, $\Delta n = 0.22$; D = 2.16, $\theta_\perp = 51°$. The patterns were obtained from structures with $n_1 = 3.6$, $\lambda = 0.9\ \mu$m and TE polarized beams.

intensity, the Gaussian approximation appears to be a very good estimate of the far-field intensity profile.

Since the beamwidth Gaussian approximation does not apply for structures with $D < 1.5$, we expect that for the same D range a Gaussian curve cannot closely fit the far-field pattern. For comparison we show in Fig. 7 a Gaussian curve with $\theta_{1/2} = 11°$ superposed over the far-field distribution of a laser with $\theta_\perp = 22°$.[38] While there is fairly good agreement from the peak intensity to its half-height (−3 dB), below −3 dB the Gaussian curve severely underestimates the far-field distribution. Similar results were obtained when comparing Gaussian curves to numerically calculated far-field patterns of structures with beamwidths below 30° and $D < 1.5$.[1] One is left with the alternative of using the Fourier transform. For $\theta < 45°$ and $D < 1.5$, it can be shown that the near-field distribution Fourier transform[28] can be simplified; as a result, the relative far-field intensity distribution is

$$\frac{I(\theta)}{I(0)} = \cos^2\theta \left(\frac{\psi' \psi^2 (2\psi' - A^2)}{2(\psi^2 - A^2)(\psi'^2 + A^2)} \right)^2 ; \; D < 1.5, \theta < 45°, \quad [25]$$

where $A = (2\pi/\lambda)\, d \sin\theta$, $\psi' = D \sin(\psi/2)$, and for ψ one can use the approximation formula obtained in Section 3 (i.e., $\psi = 4(\sqrt{1 + (D^2/2)} - 1)/D$). For various low beamwidth data we find that the condition $\theta < 45°$ is equivalent to $\theta_\perp < 40°$ if $\theta = 45°$ corresponds to a −10 dB drop in peak intensity (i.e., if $I(45°)/I(0) = 0.1$). In Fig. 7, we compare the approximation Eq. [25] to the experimental far-field with $\theta_\perp = 22°$, and find a very good agreement.

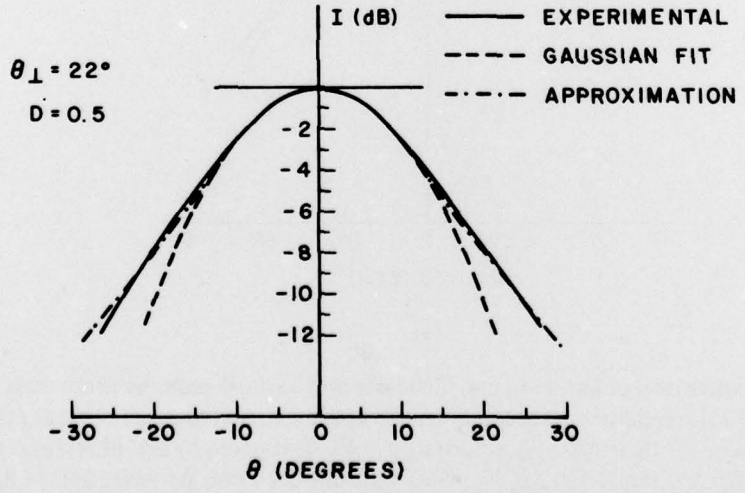

Fig. 7—Comparison of experimental (solid curves) far-field patterns of a low-beamwidth TE polarized laser ($\theta_\perp = 22°$)[38] to a Gaussian of same full-width at half-power (dashed curves), and to a Fourier transform approximation (dash-and-dot curve) for angles $\theta < 45°$ (see Eq. [25]). The structure has $D = 0.5$ and $\Delta n = 0.18$.

The far-fields (beamwidth and intensity profiles) for TM_0 modes are not treated due to the difficulty in calculations and lack of experimental data. However, from the work of Butler and Kressel[1] it turns out that, for the same DH structure, there are only slight differences between TE_0 and TM_0 mode patterns. Thus the above approximations for far-fields should be reasonable estimates for TM_0 modes as well.

For optical communications, the far-field intensity pattern determines the coupling efficiency to optical fibers when no lenses are used. It appears from our analysis that for low-numerical-aperture fibers (i.e., those of acceptance angles less than 20°), a Gaussian description of the laser beam in the plane perpendicular to the junction is fairly accurate. Then, if the laser oscillates in a fundamental lateral mode, the whole beam could be considered Gaussian. When lenses are used such that the lasing spot is imaged onto the fiber end, the degree to which the imaged field is Gaussian-like, as well as the ratio of its spot size to the fiber core radius or to the fiber spot size[27,39,40] definitely influences the coupling efficiency.

9. Conclusion

This paper contains a series of relatively simple yet very accurate analytical approximations for parameters characterizing the near- and far-field distributions of the TE_0 mode in symmetric DH lasers. For the reader's convenience we have summarized all these approximations in Table 1. As can be seen, all parameters of interest can be written as functions of only two quantities: the normalized waveguide thickness, D, and the square root of the difference in real parts of the layers' dielectric constants $\sqrt{n_1^2 - n_2^2}$. Aside from obvious simplifications in the calculation of various device parameters, the approximations should allow explicit analytical solutions for various laser optimization problems as well as physical insights into trends in device behavior. The ability to approximate near- and far-field TE_0 mode intensity patterns by a Gaussian function (over certain ranges of D and Δn) should prove useful for solving problems of scattering, radiation loss, and/or coupling to optical fibers.

The various formulae contained in the paper, together with the analytical approximations for the radiation confinement factor Γ_0[9] (i.e., $\Gamma_0 \cong D^2/(2 + D^2)$) and the mode reflection coefficient R_0[41] give a complete analytical picture for the TE_0 mode propagation inside and outside the laser. As mentioned previously, similar approximation methods can be extended to the TM_0 mode propagation in symmetric waveguides and/or fundamental mode propagation in asymmetric waveguides, by starting from their corresponding characteristic equations (Tables 2 and 3).

Acknowledgements

The author gratefully acknowledges the kind assistance of M. Ettenberg, J. K. Butler, H. Kressel and H. S. Sommers in supplying some of their calculated and experimental results. He also thanks them and C. J. Nuese for helpful discussions.

References:

[1] H. Kressel and J. K. Butler, *Semiconductor Lasers and Heterojunction LED's,* Academic Press, New York, 1977; and J. K. Butler and H. Kressel, "Design Curves for Double-Heterojunction Laser Diodes," *RCA Review,* **38,** p. 542, 1977.

[2] M. B. Panish, "Heterostructure injection lasers," *Proc. IEEE,* **64,** p. 1512, Oct. 1976.

[3] Y. Nannichi, "Recent Progress in Semiconductor Lasers," *Jpn. J. Appl. Phys.,* **16,** p. 2089, Dec. 1977.

[4] W. W. Anderson, "Mode confinement and gain in injection lasers," *IEEE J. Quantum Electron.,* **QE-1,** p. 228, Sept. 1965.

[5] D. Marcuse, *Light Transmission in Optics,* Van Nostrand Reinhold, New York, 1972.

[6] D. Botez and M. Ettenberg, "Beamwidth Approximations for the Fundamental Mode in Symmetric Double-Heterojunction Lasers," *J. Quantum Electron.,* **QE-14,** p. 827, Nov. 1978.

[7] J. F. Lotspeich, "Explicit general eigenvalue solutions for dielectric slab waveguides," *Appl. Optics,* **14,** p. 327, Feb. 1975.

[8] W. P. Dumke, "The angular beam divergence in double-heterojunction lasers with very thin active regions," *IEEE J. Quantum Electron.,* **11,** p. 400, July 1975.

[9] D. Botez, "Analytical Approximation of the Radiation Confinement Factor for the TE_0 Mode of a Double Heterojunction Laser," *IEEE J. Quantum Electron.,* **14,** p. 230, April 1978.

[10] W. B. Joyce, "Analytic approximations for the Fermi energy in (AlGa)As," *Appl. Phys. Lett.,* **32,** p. 680, May 1978.

[11] P. K. Tien, "Integrated optics and new wave phenomena in optical waveguides," *Rev. Modern Phys.,* **49,** p. 361, April 1977.

[12] T. Ikegami, "Reflectivity of Mode at Facet and Oscillation Mode in Double-Heterostructure Injection Lasers," *IEEE J. Quantum Electron.,* **QE-8,** p. 470, (1972).

[13] R. W. Davies and J. H. Walpole, "Output Coupling for Closely Confined $Pb_{1-x}Sn_xTe$ Double-Heterostructure Lasers," *IEEE J. Quantum Electron.,* **QE-12,** p. 291, May 1976.

[14] H. Kogelnik, "An Introduction to Integrated Optics," *IEEE Trans. Microwave Theory and Tech.,* **MTT-23,** p. 1, Jan. 1975.

[15] D. D. Cook and F. R. Nash, "Gain induced guiding and astigmatic output beam of GaAs lasers," *J. Appl. Phys.,* **46,** p. 1660, April 1975.

[16] T. L. Paoli, "Waveguiding in a stripe-geometry junction laser," *IEEE J. Quantum Electron.,* **QE-13,** p. 662, Aug. 1977.

[17] F. K. Reinhart, I. Hayashi, and M. B. Panish, "Mode Reflectivity and Waveguide Properties of Double-Heterostructure Injection Lasers," *J. Appl. Phys.,* **42,** p. 4466, Oct. 1971.

[18] H. C. Casey, M. B. Panish, and J. L. Merz, "Beam Divergence of the Emission from Double-Heterostructure Injection Lasers," *J. Appl. Phys.,* **44,** p. 5470, 1973.

[19] B. W. Hakki and T. L. Paoli, "Gain Spectra in GaAs Double-Heterostructure Injection Lasers," *J. Appl. Phys.,* **46,** p. 1299, March 1975.

[20] M. J. Adams, "The Cladded Parabolic-Index Profile Waveguide: Analysis and Application to Stripe-Geometry Lasers," *Opt. and Quantum Electron.,* **10,** p. 17, 1978.

[21] B. W. Hakki and F. R. Nash, "Catastrophic Failure in GaAs Double Heterostructure Injection Lasers," *J. Appl. Phys.,* **45,** p. 3907, Sept. 1974.

[22] P. A. Kirkby and G. H. B. Thompson, "Channeled substrate buried heterostructure GaAs-(AlGa)As injection lasers," *J. Appl. Phys.,* **47,** p. 4578, Oct. 1976.

[23] D. Botez and P. Zory, "Constricted double heterostructure (AlGa)As diode lasers," *Appl. Phys. Lett.,* **32,** p. 261, Feb. 1978.

[24] T. Tsukada, "GaAs-$Ga_{1-x}Al_xAs$ buried heterostructure injection lasers," *J. Appl. Phys.,* **45,** p. 4899, Nov. 1974.

[25] T. Kajimura, K. Saito, N. Shige, and R. Ito," Leaky-mode buried-heterostructure AlGaAs injection lasers," *Appl. Phys. Lett.,* **30,** p. 590, June 1977.

[26] M. Osinski, "Epstein-layer and dielectric-slab electromagnetic models of semiconductor injection lasers," *Optic and Quantum Electron.,* **9,** p. 361, Sept. 1977.

[27] D. Marcuse, "Gaussian approximation of the fundamental modes of graded-index fibers," *J. Opt. Soc. Am.*, **68,** p. 103, Jan. 1978.

[28] P. A. Kirkby and G. H. B. Thompson, "The effect of double heterostructure waveguide parameters on the far-field emission patterns of lasers," *Opto-Electron.*, **4,** p. 323, 1972.

[29] P. J. DeWaard, "Calculation of the far-field halfpower width and mirror reflection coefficients of double-heterostructure lasers," *Electron Lett.*, **11,** p. 11, 1975.

[30] K. Utaka, K. Kishino, and Y. Suematsu, "Twin-Guide Laser with Narrow Radiation Angle," *Jpn. J. Appl. Phys.*, **17,** p. 751, April 1978.

[31] G. A. Hockham, "Radiation from a solid-state laser," *Electron Lett.*, **9,** p. 389, 1973.

[32] L. Lewin, "Obliquity-factor correction to solid-state radiation patterns," *J. Appl. Phys.*, **46,** p. 2323, May 1975.

[33] J. K. Butler and J. Zoorofchi, "Radiation fields of GaAs-(AlGa)As injection lasers," *J. Quantum Electron.*, **QE-10,** p. 809, Oct. 1974.

[34] H. Kogelnik and T. Li, "Laser Beams and Resonators," *Proc. IEEE,* **54,** No. 10, p. 1312, Oct. 1966.

[35] A. Yariv, *Introduction to Optical Electronics,* Holt, Reinhart and Winston, New York, 1971.

[36] H. Kressel and M. Ettenberg, "Low-threshold double-heterojunction AlGaAs/GaAs laser diodes: Theory and experiment," *J. Appl. Phys.*, **47,** p. 3533, Aug. 1976.

[37] J. K. Butler, H. S. Sommers, Jr., and H. Kressel, "High-Order Transverse Cavity Modes in Heterojunction Diode Lasers," *Appl. Phys. Lett.*, **17,** p. 403, Nov. 1970.

[38] H. S. Sommers, Jr., private communication.

[39] W. A. Gambling, D. N. Payne, and H. Matsumura, "Mode Excitation in a Multimode Optical-Fiber Waveguide," *Electron Lett.*, **9,** p. 412, Sept. 1973.

[40] S. Nemoto and G. L. Yip, "Excitation of Self-Focusing Optical Fibre by Gaussian Beam," *Electron Lett.*, **10,** p. 150, May 1974.

[41] L. Lewin, "A Method for the Calculation of the Radiation-Pattern and Mode-Conversion Properties of a Solid-State Heterojunction Laser," *IEEE Trans. Microwave Theory and Tech.*, **MTT-23,** No. 7, p. 576, July 1975.

[42] D. Botez, "Single-Mode CW Operation of 'Double-Dovetail' Constricted DH (AlGa)As Diode Lasers," *Appl. Phys. Lett.*, **33,** p. 872, 15 Nov. 1978.